UNREINFORCED BRICK MASONRY WALL COLLAPSE INVESTIGATION UNDER OUT-OF-PLANE DYNAMIC LOADING

J.A. Prieto [(3)], A. Aviram [(1)], J.W. Badillo [(2)], J.D. Jaramillo [(4)]

[(1)] *Ph.D., P.E. (CA), Structural Engineering Independent Consultant, Lima, Peru, ady.aviram@gmail.com*
[(2)] *M.S., Doctoral Student, Civil Engineering Department, EAFIT University, Medellin, Colombia, jwbadillop@eafit.edu.co*
[(3)] *Ph.D., P.Eng., Professor, Civil Engineering Department, EAFIT University, Medellin, Colombia, jprieto7@eafit.edu.co*
[(4)] *Ph.D., Professor, Civil Engineering Department, EAFIT University, Medellin, Colombia, jjarami@eafit.edu.co*

Abstract

Several analytical methodologies used for the collapse assessment of an unreinforced brick masonry (URM) wall subjected to out-of-plane dynamic loading are presented in this paper. The URM wall was constructed in an industrial facility in Medellin, Colombia, with intermediate, lightly-reinforced and widely-spaced concrete frames resulting in large masonry panels. Although the collapse occurred during a moderate wind storm, the analytical assessment considers an equivalent triangular force distribution that could also correspond to inertial forces produced under seismic excitation. The analytical models used to investigate the wall's response to out-of-plane loading include: 1) a rigid cantilever model of masonry panels; 2) a deformable cantilever model of concrete columns; 3) deformable frame models of intermediate concrete columns and beams at mid-height with and without masonry contribution to out-of-plane bending resistance; and 4) a finite element model with all concrete frame elements, masonry units and panel openings modeled explicitly. In the latter model, different boundary conditions are used to estimate peak force and deformation demands on main wall components. Comparison of analysis results between the different models is presented in terms of out-of-plane peak deflections at the wall top, as well as peak force and stress demand-to-capacity ratios on concrete frames and masonry elements, respectively.

Past investigations on the performance of vulnerable URM walls under dynamic out-of-plane loading including wind, seismic, and blast demands, have been relatively scarce. Corresponding experimental data have primarily been derived from support motion simulating earthquakes, and quasi-static monotonic testing using airbags or multiple load points approximating distributed wind or blast pressures, or seismic inertial forces. In many of these studies, walls were not cantilevered but rather had two or more supports. Furthermore, tested walls had relatively small dimensions (i.e., length-to-width and height-to-thickness ratios) and were typically treated as rigid or semi-rigid components with idealized pinned supports. The current study is therefore a unique opportunity to evaluate the adequacy of simplified analytical methodologies to identify the collapse hazard of a long and slender URM wall under dynamic loading. Video evidence for the collapsed wall shows some degree of rotational restraint at the wall's base and significant curvatures prior to collapse in both horizontal and vertical bending directions, differing from the idealized boundary conditions and assumed deformed shapes used in past studies.

Despite significant differences between the analytical models considered in the current study, recommended parameters and assumptions lead in all cases to the correct determination of the wall's imminent collapse under the estimated demands. Equivalent static force distributions, P-Delta effects, interaction and relative contribution to the out-of-plane bending resistance of concrete framing and masonry elements with either one- or two-way action are shown to be the main parameters affecting results and governing failure modes, in addition to model selection. Recommendations for the maximum allowable wall height resulting in stable behavior are made considering only wall geometry and anticipated peak dynamic demands.

Keywords: unreinforced brick masonry; out-of-plane capacity; dynamic loading; wall collapse; slender wall instability

1. Introduction

A long and slender 2-story, 6-bay unreinforced brick masonry wall (brick URM wall) connecting two warehouse buildings in Medellin, Colombia, collapsed in 2017 during a moderate wind storm. The URM wall, constructed only a few years prior and showing some degree of distress prior to the collapse, consisted of large masonry panels separated by intermediate and lightly-reinforced concrete frames, as shown in Fig. 1. Falling debris destroyed adjacent parked vehicles and caused disruption in labor activities. Due to the high occupancy at the adjacent industrial buildings, numerous videos and photographs were taken during the collapsing wind storm, but no injuries were reported. The wall prior and following the collapse is shown in Fig. 2, where wall perforations at the top half of the wall were added at an unknown date.

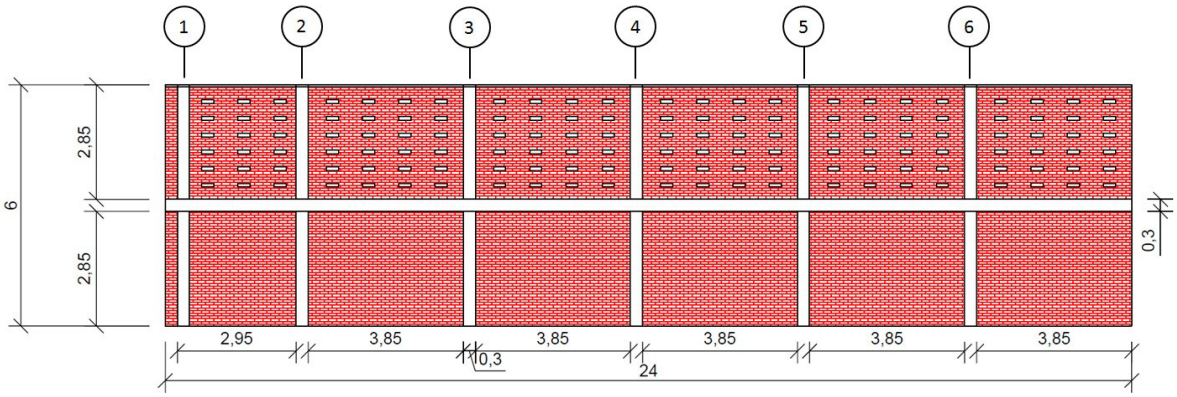

Fig. 1. – Wall geometry prior to collapse. Wall thickness is 14.6 cm, dimensions shown are in meters [1, 2].

Fig. 2. – Brick URM wall prior to the collapse and resulting debris pattern (below) [1, 2] Gridlines 1-6 run from right to left in both photos.

The collapse sequence and resulting debris pattern obtained from a video recording taken near gridline 1 is shown in Fig. 3. The recording displays large wall deflections in both horizontal and vertical bending directions, as well as the initiation of the collapse due to failure of end supports (i.e., left and right vertical edges) towards the wall top. The loss of the wall end supports then resulted in masonry panel diagonal failure near gridline 1, failure of concrete column base supports acting in cantilever action, and global wall instability due to large deflections.

Fig. 3. – Collapse sequence obtained from video recording [1].

Due to informal construction practices in the region, design calculations and material specifications were not available for this study. However, construction drawings, photographic, video, and limited forensic evidence were available for examination, along with regional wind velocity measurements at the time of collapse. Since the remaining debris was quickly removed from the site following the collapse, proper material sampling was not feasible. Therefore, material strength data is estimated in this study by surveying local brick manufacturers. Specific information regarding brick geometry, construction details, and material data can be found elsewhere [1, 2].

Past investigations on the performance of URM walls under dynamic out-of-plane demands have been relatively scarce and related work on other masonry structures included support motion simulating earthquake and blast loads [3, 4]. Experimental data on URM walls under out-of-plane demands have primarily been derived from quasi-static and monotonic testing using airbags or multiple load points approximating distributed wind or blast pressures, or seismic inertial forces [5-9]. In many of these studies, walls were not cantilevered but rather had two or more supports. Furthermore, tested walls had relatively small dimensions (i.e., length-to-width and height-to-thickness ratios) and were typically treated as rigid or semi-rigid components with idealized pinned supports, which could differ from actual site conditions.

The current study is therefore a unique opportunity to evaluate the adequacy of several simplified analytical methodologies to identify the collapse hazard of a long and slender URM wall under dynamic loading. The collapsed wall height-to-thickness and length-to-height ratios of 40 and 4, respectively, are significantly higher than experimentally-tested URM wall specimens found in literature. Furthermore, since video evidence of the collapsed wall shows some degree of rotational restraint at the wall base and significant curvatures prior to collapse in both horizontal and vertical bending directions, these conditions differ from the idealized boundaries and assumed deformed shapes used in past studies. Comparison of analysis results is presented herein in terms of out-of-plane wall deformations, as well as demand-to-capacity force and stress ratios (DCRs) in concrete and masonry elements, respectively. While the focus of many past studies was localized wall deformations leading to the formation of a single primary crack at the masonry-mortar interface at the point of maximum bending demand and governing flexural capacity, the current evaluation utilizes global stability and wall displacement estimates.

2. Collapse Investigation

2.1 Applicable design codes

For the collapsed URM wall assessment local and international design codes are used in this study. Among them are the Colombian Seismic Resistant Construction Code NSR-10 [10], specifically Title B Loads, Title C Structural Concrete, and Title D Structural Masonry, the Colombian Technical Norm NTC 2289 for reinforcing steel [11], the US codes ACI 318-11 for reinforced concrete frames [12], and TMS 402/602 for masonry design [13]. The wall system is conservatively categorized in this study as unreinforced masonry instead of confined masonry in-filled in concrete frames due to several reasons: 1) wind loads are imposed in the out-of-plane dimension and concrete frames do not provide confinement under these actions, 2) masonry panel dimensions are relatively large, and 3) there is no beam at the wall top but rather a mortar architectural detail.

2.2 Loading data

Wind demands are estimated through triangular spatial interpolation of actual wind measurements in the Medellin region at the time of collapse recorded by SIATA, the local meteorological institute [14]. Recorded peak gusts at 13 nearby stations ranged from 4.5 to 14.2 m/sec, and the spatially interpolated peak gust speed at the wall site is determined at 12.3 m/sec. Per NSR-10 [10], the Medellin region is located in wind risk category 4 (out of 5) with a basic design wind velocity of 33 m/sec (120 km/h). The estimated peak gust speed at the time of the wall collapse was therefore clearly well below the design value, indicating the wall was under-designed for wind loads.

For the corresponding site conditions, peak wind pressure is estimated using the Analytical Procedure of NSR-10 Chapter B.6 [10] as q_{max}=100 Pa. While in reality a parabolic wind pressure distribution develops on the wall due to increasing wind velocity above ground level, analytical results corresponding to an idealized triangular force distribution is presented in this paper. The triangular force distribution and analytical methodologies presented can be similarly applied in seismic analysis of URM walls with similar characteristics. Calculations of the wind pressure and additional results obtained from a more critical uniform pressure distribution can be found elsewhere [1, 2].

2.2 Observed response

Using video evidence recorded from two different angles at the time of collapse, the wall top peak deflections at incipient collapse are estimated between 15 and 20 cm. These peak deflections are estimated at the wall top between gridlines 4 and 5, as shown in Fig. 1. and Fig. 3. At this peak displacement, the columns at gridlines 2-6 in Fig. 1 and adjacent masonry panels displayed partial rotational restraint at the base, according to video evidence [1]. The masonry panels also presented a curved deformed shape in both bending directions (see Fig. 3). The collapse sequence and debris pattern also reveal that once the horizontal supports at the wall ends failed, the concrete columns and masonry panel bases in cantilever action were unable to resist the sustained

wind pressures, and the entire system underwent large displacements and jointly rotated towards the ground resulting in the debris pattern in Fig. 2.

3. Brick URM Wall Analysis Methodology

Several simplified analytical approaches with different basic assumptions and complexity levels are used in the wall collapse investigation to approximate wall out-of-plane deflections and DCRs in concrete frames and masonry elements. These include: 1) a rigid cantilever model of masonry panels; 2) a deformable cantilever model of concrete columns; 3) deformable frame models of intermediate concrete columns and beams at mid-height with and without masonry contribution to out-of-plane bending resistance; and 4) a finite element model with all concrete frame elements, masonry units and panel openings modeled explicitly. The general scheme and corresponding wind demands under triangular pressure distribution is presented for each method in the following subsections and in Fig. 2-4. As previously mentioned, uniform pressure distribution is also considered in this study but is presented elsewhere [1, 2].

The Rigid Cantilever and Deformable Cantilever models accounting solely for the concrete columns are assessed through hand calculations, while the Frame wall models, assessed in the structural analysis program SAP2000 are modeled with and without masonry contribution to wall out-of-plane bending stiffness and strength. The effective masonry width is taken as 6 times the wall thickness on either side of the column, in accordance with NSR-10 [10] for out-of-plane loading of masonry with running bond.

3.1 Rigid Cantilever model

In past investigations, cracked URM walls rocking with large horizontal displacements due to out-of-plane wind or seismic loading have been modeled as rigid blocks separated by fully cracked cross-sections [5, 8]. This assumption is realistic if there is no vertical pre-compression to deform the blocks, the supports are cracked and allow for simultaneous wall-support rotation, and the dynamic response of the system resembles that of the first mode of vibration. The class of URM walls satisfying such conditions include cantilever walls and simply supported walls spanning vertically, with an additional idealized hinge at mid-height.

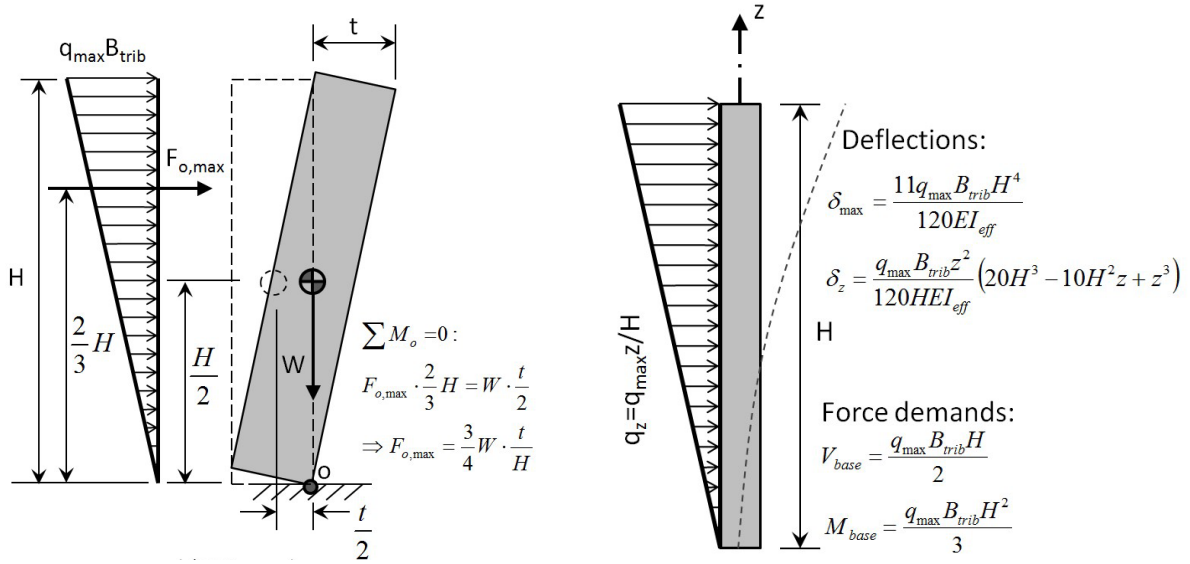

(a) Rigid Cantilever model at incipient rocking (b) Deformable Cantilever model

Fig. 4. – Cantilever wall models [1].

In this study dynamic wind loading is applied as a triangular static force or pressure, while inertial forces are ignored, according to the scheme shown in Fig. 4(a). Bending moment equilibrium around the pivot point at the wall base enables the determination of the maximum allowable wind force on the wall before it becomes

unstable. At incipient collapse, the wall center of mass is displaced horizontally beyond the projected pivot point, resulting in wall overturning. In this formulation, the displacement capacity at incipient collapse of 14.6 cm is solely based on wall thickness whereas the strength capacity, assessed separately, is significantly influenced by assumed boundary conditions.

3.2 Deformable Cantilever model

Neglecting the contribution of masonry units and mid-height beam to wall stiffness and strength, the Deformable Cantilever model solely includes the concrete column resistance. These columns are assumed to be fully fixed at the base and free to translate and rotate at the top. Cracked cross section properties are used for the effective out-of-plane bending stiffness. While ACI 318-11 [12] recommends the use of a 0.35 reduction factor to column elements with low gravity loads under bending demands, a 0.25 reduction factor is used instead, i.e., $E_cI_{c,effective}=0.25E_cI_{c,gross}$, where I_c is the column moment of inertia in the vertical bending direction. This is due to significantly visible cracking observed through photographic evidence prior to collapse and low reinforcement ratio. The tributary width in the computation of distributed wind demands on each column is taken as half the distance between adjacent columns. The shear, bending moment, and deformation demands are computed using simple beam equations, as shown in Fig. 4(b), while P-Delta effects are neglected in this simplified modeling approach.

In this model, for a mid-height deflection demand equal to half the wall thickness, the wall top deflection is computed as approximately 20 cm for the triangular load distribution. This indicates that if column resistance and base fixity were adequate, the wall top could have deflected as much as 20 cm without resulting in overturning due to P-Delta effects.

3.3 Frame models

The horizontal beam contribution to wall out-of-plane bending resistance is examined in the Frame models, shown in Fig. 5, using SAP2000 Version 19.2.1 structural analysis program. The Frame Model Without Masonry Contribution assumes the concrete frames support the masonry and concrete tributary weight, as well as the tributary wind pressures. The columns are assumed to be fully fixed at the base while the beam is assigned pinned supports at wall ends. Frame element cracked cross section properties are defined similarly as in the Deformable Cantilever model. In the Frame Model with Masonry Contribution equivalent masonry frame elements are added in parallel to concrete columns, as shown in Fig. 5, while masonry contribution to concrete beams is ignored.

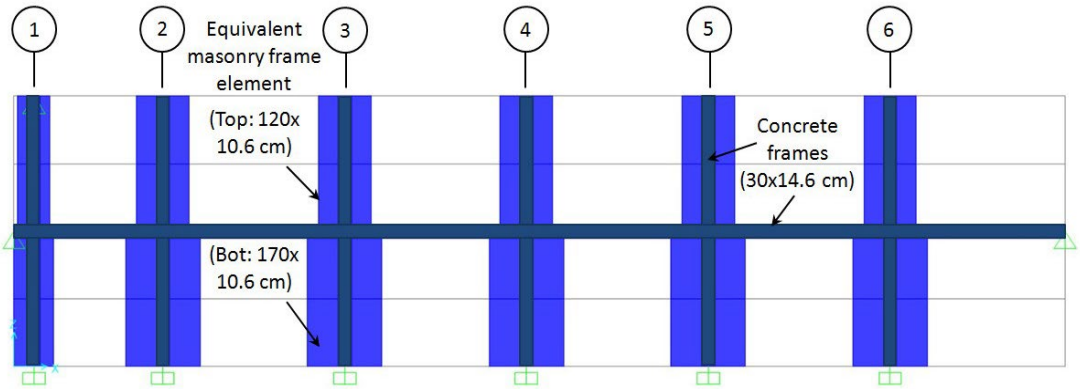

Fig. 5. – Frame model with or without masonry contribution [1, 2].

In the latter model, for the wall bottom half the effective masonry width is taken as 6 times the wall thickness (or 85 cm) on either side of the column, in accordance with NSR-10 Section D5.4.4 [10] for out-of-plane loading of masonry with running bond. The effective width for the wall top half is estimated as the distance from the column edge and the center of the closest wall openings (or 60 cm) located on either side of the column. The equivalent thickness of a solid masonry section resisting out-of-plane bending and shear demands is calculated as 10.6 cm from the hollow 14.6 cm deep masonry units in the out-of-plane bending

direction and 1 to 2 cm thick vertical mortar joints connecting the units. The masonry elastic out-of-plane bending inertia, I_m, is significantly reduced in the model by a factor of 0.1, i.e., $E_mI_{m,eff}=0.1E_mI_{m,gross}$, assuming the lack of reinforcement and grouting would lead to significant cracking prior to collapse. Adverse P-Delta effects are included in the analysis, resulting in increased overturning demands due to the wall's self-weight.

3.4 Finite Element model

The Finite Element (FE) model developed for this study is also analyzed using SAP2000 Version 19.2.1 and includes explicit modeling of concrete frames, masonry units and panel openings to assess the resulting out-of-plane bending resistance to dynamic loading, as shown in Fig. 6. Finite element mesh size are defined using a preliminary mesh sensitivity analysis. The thickness of the equivalent solid masonry shell elements is determined using a similar methodology to the one employed in the Frame models to match the hollow brick masonry elastic section modulus, including the contribution of mortar joints. In this model, however, the average thickness calculated for the two main bending directions (i.e., m_{11} and m_{22}) is used, due to differences in the cross sections of the hollow brick unit and spacing of horizontal and vertical joints.

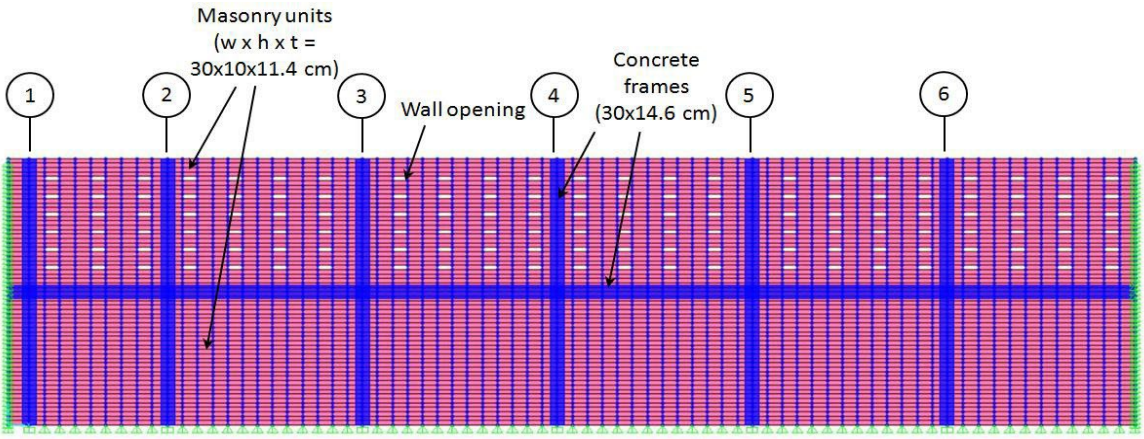

Fig. 6. – Finite Element model accounting for two-way bending of masonry panels [1, 2].

Similar to the Frame models, the FE model uses effective section properties in flexure due to considerable cracking observed prior to the collapsing event, specifically $0.25E_cI_{c,gross}$ for concrete elements, and $0.1E_mI_{m,gross}$ for masonry under out-of-plane bending. The model includes two-way bending of masonry panels (i.e., m_{11} and m_{22} shell element properties multiplied by 0.1 factor) and concrete frames (i.e., I_{22} out-of-plane frame bending inertia multiplied by 0.25) but no membrane resistance of the masonry in tension (i.e., f_{11}, f_{12}, and f_{22} shell element properties multiplied by 0).

Gravity loads corresponding to masonry self-weight (i.e., membrane response in compression) are applied as tributary distributed loads on columns and beams, similar to the methodology used in the Frame models, to include P-Delta effects on the wall overturning demands. The modeling of concrete frames, effective cross section properties, tributary gravity loads, and boundary conditions in the Finite Element model are identical to those used in the Frame models.

Dynamic wind loads are applied in the FE model as static pressure on masonry shell elements that transfer the load to the columns. The FE model shown in Fig. 6 includes two different boundary conditions: 1) restrained vertical wall edges for estimation of stress demands at end supports and 2) unrestrained vertical wall edges for estimation of peak deflections at wall top and bending demands at wall base. Fig. 7 showing FE analysis force results clearly illustrates the considerable effect of these two sets of boundary conditions on the overall wall behavior. When end supports at vertical edges are applied (i.e., prior to support failure), horizontal bending demand of masonry panels spanning between intermediate concrete columns, combined with global wall bending as a simply-supported beam measuring 24 m long, govern the peak force and deformation demand, as well as the corresponding failure modes. Once these supports fail or are removed from the FE model, wall bending in the vertical direction acting as a cantilever measuring 6 m long, then governs the

response. The high deflection demands of the cantilever results in high force demand exceeding element capacity and wall instability resulting in collapse.

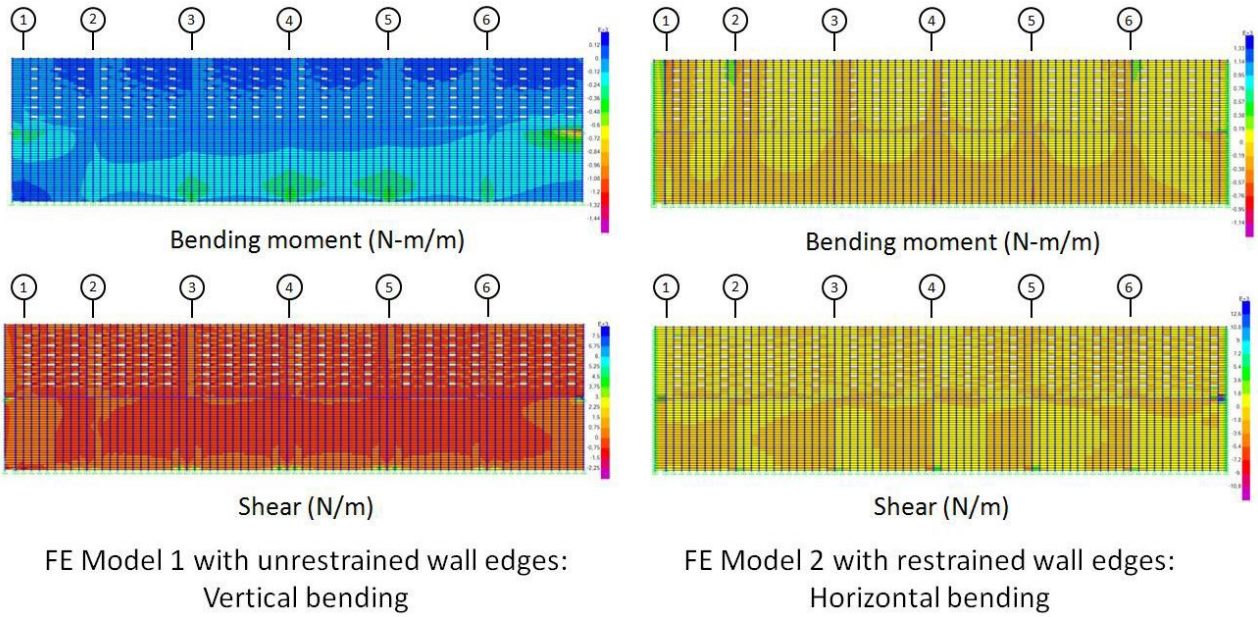

Fig. 7. – Finite Element model force results under triangular wind pressure [1].

3. Wall Capacity Estimation

The ultimate concrete column capacity including axial compression, out-of-plane bending moment and shear resistances is calculated using ACI 318-11 [12] and NSR-10 Title C Structural Concrete [10], and is presented in Table 1. For axial compression, the assumed lateral restraint conditions and global wall slenderness varies between the different analytical models, as described previously. Since P-Delta effects and column slenderness are explicitly included in the Frame model and analysis, the resulting column moment demand magnification is computed directly, while the applied axial load is limited by column cross section axial capacity, as per ACI 318-11 [12].

Table 1 – Concrete frame capacities.

Analytical Model	Beam/Column		Column		Beam
	Moment (kN-m)	Shear (kN-m)	Slenderness ratio	Axial compression (kN)	Axial tension (kN)
Deformable Cantilever Frame Finite Element	6.31	16.5	Kh'/r=300 Sway frame	696 (max)	106

The frame section capacities approximated for the deformable analytical model conservatively assume similar boundary conditions for the columns in all models. The calculated shear capacity only includes the contribution of the concrete section, reduced by half per ACI 318-11 [12], since no transverse reinforcement

was provided for out-of-plane bending. The beam's flexure and shear capacities are identical to the column's, and the ultimate axial tensile capacity only includes the contribution of steel reinforcement.

The masonry capacity assessment is carried out using NSR-10 Appendix D-1 and the Allowable Stress Design (ASD) method, as specified in NSR-10 for unreinforced masonry and as presented in Table 2. The allowable axial stress, tensile and compressive stresses due to bending, and shear stress are estimated considering both vertical and horizontal bending of the masonry panels. The allowable axial stress, F_a, is calculated as a function of the slenderness reduction factor, R_e. The allowable compressive stress due to bending, F_b, is calculated as a function of the concrete compressive strength, f'_m. The allowable tensile stress due to bending, F_t, is estimated as 0.10 MPa and 0.21 MPa for stresses perpendicular to horizontal and vertical mortar joints in unreinforced ungrouted masonry, respectively. The allowable shear stress, F_v, is calculated as a function of both the masonry compressive strength, f'_m, and the compressive stress due to Dead Load, f_{am}.

Table 2 – Unreinforced brick masonry allowable stress (MPa).

Analytical Model	F_a	F_b	F_t	F_v
Frame with Masonry Contribution; Finite Element	0.16 (R_e=0.26)	0.99	0.21 (vertical joints) 0.10 (horizontal joints)	0.04 (no axial compression) 0.07 (axial compression at base)

4. Analysis Results

4.1 Peak deflections

Despite experiencing nonlinear deformations under dynamic wind loading, out-of-plane wall deflections are calculated in this study assuming linear-elastic behavior with an effective stiffness in all models. Several iterations and parameter variations are required to achieve reasonable precision. The wall top peak calculated, and allowable out-of-plane lateral deflections vary between the models, as shown in Table 3, due to different modeling assumptions such as deformed shapes and boundary conditions.

Table 3 – Peak and allowable lateral deflections at wall top (triangular pressure distribution).

Model	Wall top deflection (cm)		Boundary Conditions	Unstable? (Y/N)
	Computed	Allowable		
Rigid Cantilever	$>\Delta_{all}$*	14.6	Pinned bottom, free top	Y
Deformable Cantilever	19.6	20.3	Fixed bottom, free top	N
Frame Without Masonry Contribution	16.1	20.3	Fixed bottom, free top	N
Frame With Masonry Contribution	13.9	20.3	Fixed bottom, free top	N
Finite Element	8.4	11.3	Pinned bottom, rotational restraint top	N

*Δ_{all}- Allowable deflection resulting in incipient collapse reached at $q=48\ Pa \ll q_{max}$

The allowable deflection at the wall top corresponds to a mid-height deflection equal to half the wall thickness, beyond which the wall's center of mass contributes to overturning and collapse. In this formulation, the triangular pressure distribution is used to compute the resulting lateral deformations. In general, as shown

in Table 3, the range of deformations demands, as well as allowable limits marking the initiation of the collapse sequence approximate fairly accurately available photographic, video, and forensic evidence. Even though the deflection results under the triangular force distribution indicate the wall theoretically remains stable, the capacity of concrete and masonry elements sustaining the corresponding force and stress demands, respectively, must also evaluated, as discussed in the next section. It is important to note that under the more critical uniform wind pressure distribution which results in higher force and deflection demands, as well as slightly lower allowable deflection values, the collapse of the wall is predicted for all assessed models.

As seen from Table 3, the stiffness contribution of the concrete beam at mid-height in the Frame Model Without Masonry Contribution resulted in an 18% reduction in lateral deflections compared to Deformable Cantilever model with different tributary widths. The added stiffness of the equivalent masonry frames in the Frame Model With Masonry Contribution resulted in a 14% reduction in lateral deflections, while the two-way bending stiffness of masonry elements in the FE model resulted in a further reduction of 40% compared to the latter model under uniform pressures, respectively.

Using this analytical procedure, a conservative estimate of the maximum wall height remaining stable under a maximum pressure, q_{max} of 100 Pa, was determined at 2.9 and 1.9 m under triangular and uniform pressure distributions, respectively.

4.2 Demand-to-capacity ratios (DCRs)

DCRs for concrete elements are estimated using wind demand results, assumed to be at the Strength Design (SD) level and amplified due to P-Delta effects. Conversely, wind demands for masonry elements are converted to Allowable Stress Design (ASD) level by using a reduction factor of 1/(1.6)0.5 per ASCE 7-10 [15] or approximately 0.79 for the different actions assessed (i.e., axial, bending, shear). No load amplification or reduction factors are applied to gravity loads since these are already assumed to be at the ASD level. Table 4 summarizes the maximum DCRs for the different analytical models in this study, the governing failure mode corresponding to the action with the highest DCR, and the determination of wall failure if controlling DCRs exceed a value of 1.0.

Table 4 – Demand-to-capacity ratios in concrete and masonry elements (DCRs).

Model	Concrete Element		Masonry Element		Fails? (Y/N)
	Max DCR	Governing Failure	Max DCR	Governing Failure Mode	
Rigid Cantilever	N/A	N/A	N/A	N/A	N/A
Deformable Cantilever	1.16	Column Flexure	N/A	N/A	Y
Frame Without Masonry Contribution	1.01	Column Flexure	N/A	N/A	Y
Frame With Masonry Contribution	0.87	Column Flexure	1.00	Compression due to Bending	Y
Finite Element	0.66	Column Flexure	1.04	Tension due to Bending	Y

As seen from Table 4, for concrete elements, the governing failure mode produced in the models is flexural failure of concrete columns at the base. Although not shown in Table 4, shear stress demands and compressive stress demands due to the masonry wall weight and bending under wind loads in the masonry panels results in DCRs that generally did not exceed a value of 1.0, and therefore are not considered the main cause of failure. Table 4 indicates that where the masonry contribution to wall stiffness and strength is directly assessed, the resulting governing failure mode leading to predicted wall collapse is the exceedance of the

allowable tensile stress due to wall bending at the base. It is important to note that all modeling schemes considered successfully determine the collapse of the wall under the assumed triangular, as well as the more critical uniform wind force distributions.

5. Conclusions and Recommendations

The collapse of a slender 2-story and 6-bay unreinforced brick masonry wall under moderate wind loads is assessed using simplified analytical approaches to evaluate their efficacy in predicting the observed behavior. Linear static analyses are used to simulate a highly nonlinear dynamic phenomenon by calibration of effective stiffness properties and the idealization of support conditions. These analysis approaches for out-of-plane URM wall response are considered adequate for nonlinear dynamic wind or seismic demands as long as the net pressure or inertial forces, respectively, act on one side of the wall and generate a deformed shape similar to the first mode of vibration. The analyses used in the current study include static application of triangular wind pressure distributions and results in force and deformation demands that closely approximate available photographic, video, and forensic evidence. A more critical and conservative uniform wind pressure distribution is also considered in the study but the results are presented elsewhere.

Among the different approaches used, the rigid masonry cantilever wall model with rocking behavior is the most conservative, predicting collapse at wind pressures significantly lower than registered. According to this method, which only required basic wall geometry as input parameters, the maximum wall height of similar construction that would resist collapse is between 2 and 3 meters, a fraction of the actual wall height of 6 meters. The other analytical models considered are a simple cantilever, frame models of concrete elements with and without masonry contribution to wall out-of-plane stiffness and strength, and a finite element model with two-way bending but no membrane resistance in tension.

The governing failure modes in the different models consist primarily of bending failure of concrete columns and exceedance of the allowable compressive and tensile stresses in masonry elements near the wall base. At vertical edges of masonry panels large stresses are also recorded due to horizontal bending between column lines and the wall's high overall length-to-height ratio. Even though the peak deflection estimation did not predict wall instability in all cases under the triangular distribution, the more critical uniform force distribution considered in the study but presented elsewhere did result in failure for all analysis models. DCR results are similar between the different models with maximum values in either concrete or masonry elements exceeding 1.0 under the triangular, as well as the uniform force distribution in all cases.

In general, the wall design proved to be deficient since collapse is predicted by all analysis methodologies considered under moderate wind speeds recorded at the site, which are considerably lower than specified regional design wind speeds. A similar collapse could have also resulted in the wall under a moderate seismic event due to high wall slenderness ratio, low out-of-plane resistance of unreinforced masonry panels, and low capacity of lightly-reinforced intermediate concrete frames.

Although the different analysis models are relatively simple, several iterations and parameter variations are required to achieve reasonable precision. Since formal design calculations are not available for this structure, as is customary in the region, the use of empirical design procedures or regional construction practices should be revised. Conservative design recommendations should be developed for unreinforced masonry walls in industrial facilities and parking structures to prevent future failures.

6. References

[1] Aviram A, Badillo JW, Prieto JA, Jaramillo JD (2019): Unreinforced brick masonry wall collapse investigation under moderate wind loads. *Revista Ingenieria de Construccion RIC,* **34** (1), 205-220.

[2] Aviram A, Badillo JW, Prieto JA, Jaramillo JD (2019): Unreinforced brick masonry wall collapse investigation under moderate wind loads. *9th Colombian National Congress of Seismic Engineering*, Cali, Colombia.

[3] Beak M, Colwell SA, Crowhurst D, and Ellis BR (1994): The behaviour of masonry and concrete panels under explosion and static loading. *I Chem E Symposium Series No.* ***134***, 227-247.

[4] Elsayed M, El-Dakhakhni W, Razavi S, Mekky W, and Tait M (2013): Response of one-way reinforced masonry walls to blast loading. *12th Canadian Masonry Symposium*, Vancouver, British Columbia, Canada.

[5] Doherty K, Griffith MC, Lam N, and Wilson J (2002): Displacement-based seismic analysis for out-of-plane bending of unreinforced masonry walls. *Earthquake Engineering and Structural Dynamics*, **31** (4), 833-850.

[6] Bean Popehn JR, Schultz AE, Lu M, Stolarski HK, and Ojard NJ (2008): Influence of transverse loading on the stability of slender unreinforced masonry walls. *Engineering Structures*, **30** (10), 2830-2839.

[7] Derakhshan H and Ingham JM (2008): Out-of-plane testing of an unreinforced masonry wall subjected to one-way bending. *Australian Earthquake Engineering Conference*, Ballarat, Victoria, Australia.

[8] Vaculik J (2012): Unreinforced masonry walls subjected to out-of-plane seismic actions (PhD Dissertation). *PhD Dissertation*, School of Civil, Environmental & Mining Engineering, University of Adelaide, Australia.

[9] Udey A (2014): Realistic wind loads on unreinforced masonry walls. *MS Dissertation*, Department of Civil and Geological Engineering. University of Saskatchewan, Saskatoon, Canada.

[10] MinAmbiente (2010): NSR-10 Reglamento Colombiano de Construcción Sismo Resistente. *Ministerio de Ambiente, Vivienda y Desarrollo Territorial (MinAmbiente)*. Asociación Colombiana de Ingeniería Sísmica, Bogotá, Colombia.

[11] ICONTEC (2007): NTC 2289 Barras Corrugadas y Lisas de Acero de Baja Aleación, Para Refuerzo de Concreto- Norma Técnica Colombiana. *Instituto Colombiano de Normas Técnicas y Certificación (ICONTEC)*, Bogotá, Colombia.

[12] ACI (2011): ACI 318-11, Building Code Requirements for Structural Concrete. *American Concrete Institute (ACI)*, Farmington Hills, MI, USA.

[13] MSJC (2011): TMS 402-11/ACI 530-11/ASCE 5-11 Building Code Requirements for Masonry Structures and TMS 602-11/ACI 530.1-11/ASCE 6-11 Specification for Masonry Structures. *Masonry Standards Joint Committee (MSJC)*, The Masonry Society, Boulder, CO, USA.

[14] SIATA (2017): *Sistema de Alerta Temprana de Medellín y el Valle de Aburra (SIATA)*. https://www.siata.gov.co/sitio_web/index.php/monitoreo#estaciones_meteorologicas.

[15] ASCE (2010). ASCE/SEI 7-10, Minimum Design Loads for Buildings and Other Structures. *American Society of Civil Engineers (ASCE)*, Reston, Virginia, USA.

